



HAL
open science

Influence of injected interstitials on α' precipitation in Fe–Cr alloys under self-ion irradiation

O. Tissot, Cristelle Pareige, E. Meslin, B. Décamps, J. Henry

► **To cite this version:**

O. Tissot, Cristelle Pareige, E. Meslin, B. Décamps, J. Henry. Influence of injected interstitials on α' precipitation in Fe–Cr alloys under self-ion irradiation. *Mater.Res.Lett.*, 2016, 5 (2), pp.117-123. 10.1080/21663831.2016.1230896 . hal-01921664

HAL Id: hal-01921664

<https://hal.science/hal-01921664>

Submitted on 29 May 2019

HAL is a multi-disciplinary open access archive for the deposit and dissemination of scientific research documents, whether they are published or not. The documents may come from teaching and research institutions in France or abroad, or from public or private research centers.

L'archive ouverte pluridisciplinaire **HAL**, est destinée au dépôt et à la diffusion de documents scientifiques de niveau recherche, publiés ou non, émanant des établissements d'enseignement et de recherche français ou étrangers, des laboratoires publics ou privés.



Influence of injected interstitials on α' precipitation in Fe–Cr alloys under self-ion irradiation

O. Tissot, C. Pareige, E. Meslin, B. Décamps & J. Henry

To cite this article: O. Tissot, C. Pareige, E. Meslin, B. Décamps & J. Henry (2017) Influence of injected interstitials on α' precipitation in Fe–Cr alloys under self-ion irradiation, Materials Research Letters, 5:2, 117-123, DOI: [10.1080/21663831.2016.1230896](https://doi.org/10.1080/21663831.2016.1230896)

To link to this article: <http://dx.doi.org/10.1080/21663831.2016.1230896>



© 2016 The Author(s). Published by Informa UK Limited, trading as Taylor & Francis Group.



Published online: 19 Sep 2016.



Submit your article to this journal [↗](#)



Article views: 152



View related articles [↗](#)



View Crossmark data [↗](#)

Influence of injected interstitials on α' precipitation in Fe–Cr alloys under self-ion irradiation

O. Tissot^{a,b}, C. Pareige^b, E. Meslin^c, B. Décamps^d and J. Henry^a

^aDEN-Service de Recherches Métallurgiques Appliquées, Laboratoire d'Analyse Microstructurale des Matériaux, CEA, Université Paris-Saclay, Gif-sur-Yvette, France; ^bNormandie Univ, UNIROUEN, INSA Rouen, CNRS, Groupe de Physique des Matériaux, Rouen, France; ^cDEN-Service de Recherches de Métallurgie Physique, CEA, Université Paris-Saclay, Gif-sur-Yvette, France; ^dCentre de Sciences Nucléaires et de Sciences de la Matière (CSNSM), Université Paris-Saclay, Orsay, France

ABSTRACT

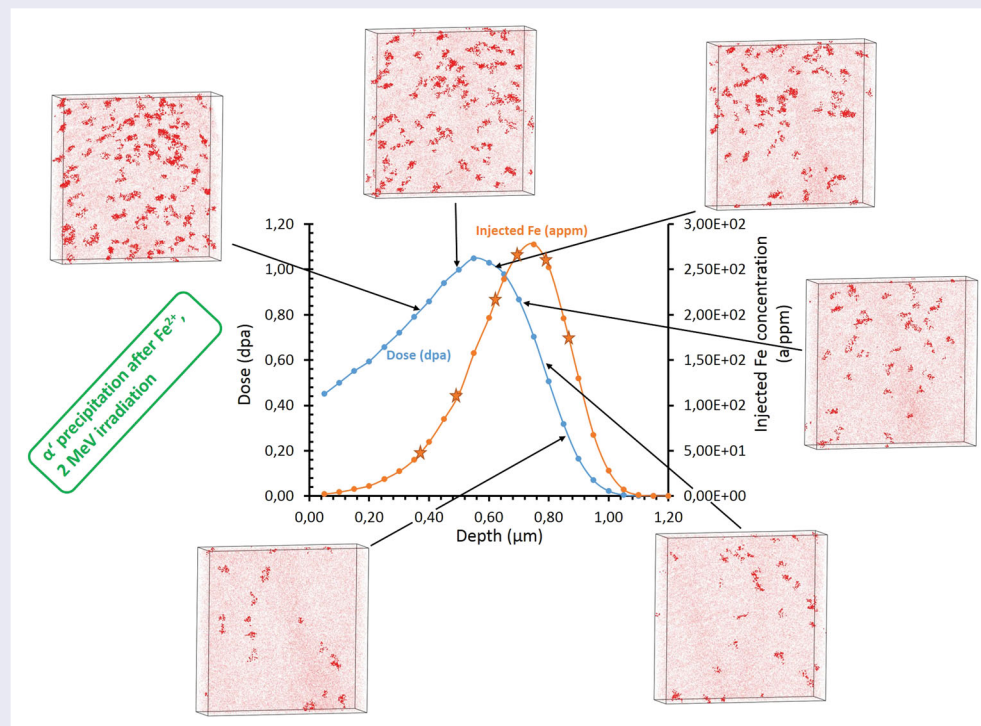
Depending on the particle used to irradiate Fe–Cr alloys, at the same dose and temperature, α' precipitation may occur or not. This paper aims at explaining the origin of the absence of α' precipitation under ion irradiation. A Fe–15at.%Cr alloy was irradiated with 2 MeV Fe^{2+} ions at 300°C and analysed using atom probe tomography. For the first time to our knowledge, α' particles were observed under ion irradiation. The characterisation of the α/α' decomposition with depth showed that injected Fe strongly reduced α' precipitation. They might have played a major role in the absence of α' precipitation under ion irradiation.

ARTICLE HISTORY

Received 11 March 2016
Accepted 26 August 2016

KEYWORDS

Fe–Cr; ion irradiation; precipitation; atom probe tomography; injected interstitials



IMPACT STATEMENT

This paper reports the first observation of α' precipitation in Fe–Cr alloys after heavy ion irradiation and demonstrates that the injected interstitial effect drastically modifies the precipitation behaviour.

High-Cr Ferritic–Martensitic steels and oxide dispersion-strengthened alloys are potential candidates for cladding and structural alloys for future GEN IV and fusion

reactors because of their excellent swelling resistance, small ductile–brittle transition temperature shift and good thermal properties [1–5]. The development and

CONTACT O. Tissot olivier.tissot@cea.fr

qualification of new structural materials, which will be subjected to an intense neutron flux, require a deep understanding of the microstructural changes operating under neutron irradiation. Nevertheless, the microstructure evolution of the steels under irradiation is very complex because of their complex initial microstructure and chemistry. Moreover, neutron irradiations are long, expensive and access to facilities is restricted. For all these reasons, the community focuses on model irradiation experiments performed on Fe–Cr model alloys using alternative irradiation sources. Alloys containing more than 12% Cr are of particular interest in nuclear plants because of their corrosion resistance, but they are prone to embrittlement due to α' precipitation below 500°C [6,7].

Ions are often used to simulate neutron damage. However, the irradiation conditions may have a pronounced effect on the alloy microstructural evolution [8]. Dose rates in the case of ion irradiation experiments are usually several orders of magnitude higher than those under neutron irradiation. The same Fe–12at.%Cr and Fe–9at.%Cr alloys were irradiated at 300°C using Fe ions at a dose rate of 2×10^{-4} dpa/s and using neutrons at a dose rate of 10^{-7} dpa/s and analysed using atom probe tomography (APT) [9,10]: α' particles were only observed under neutron irradiation. To the best of our knowledge, α' precipitation has never been reported after heavy ion irradiation at high-dose rates (10^{-3} – 10^{-4} dpa/s), whereas α' precipitation has been shown to occur via an enhanced mechanism under neutron irradiation at low-dose rates ($\sim 10^{-7}$ dpa/s) [9–16]. Nevertheless, the difference in dose rate cannot explain by itself the difference in α' precipitation. Indeed, α/α' decomposition was observed after irradiation at relatively high-dose rates ($\sim 10^{-5}$ dpa/s) with 16 MeV protons [17]. α' precipitation has also been shown to occur in an Fe–15%Cr electron irradiated with a dose rate of 3.9×10^{-5} dpa/s close to ion conditions [18]. The cascade size is also not a determining factor as α' precipitates were observed under electron irradiation, for which only Frenkel pairs are created and under proton irradiation which produces comparatively smaller size cascades than ion and neutron irradiations. The existence of a ballistic dissolution mechanism of small α' clusters could be considered as well. However, ballistic unmixing is unlikely to play an important role considering the standard dose rates (10^{-3} – 10^{-4} dpa/s) and temperature range (300–500°C) as shown by atomistic kinetic Monte Carlo calculations [19] performed assuming low sink densities. In summary, there is currently no clear understanding as to why α' precipitation has never been observed in heavy ion irradiation.

Another parameter to consider which is specific to ion irradiation is the presence of injected ions. Indeed, ions used to irradiate a thick target come to rest at the end of time range in the material as interstitial atoms and could impact diffusion process or the creation of point defect clusters, for example. Prior studies have demonstrated the significant influence of the injected Fe atoms on ion-induced swelling [20–27]. Both experimental and theoretical works showed that injected ions suppress void swelling. The effect of the injected ions on α' precipitation has never been considered up to now. The present study aims at studying this effect.

In order to gain further insight into the mechanisms that could explain the difference in the precipitation kinetics under ion irradiation and the other forms of irradiation (e.g. neutron, proton and electron), 2 MeV Fe^{2+} irradiation was performed on a high purity Fe–15at.%Cr alloy (the same alloy as in [18]). APT was used to investigate the influence of both damage and injected Fe profiles on α/α' decomposition.

The high-purity Fe–15at.%Cr alloy was prepared by induction melting at the Ecole des Mines de Saint Etienne in France. The alloy was received in a recrystallised state, after a cold reduction of 70% and 1 h at 1123 K under pure argon which was followed by air-cooling to room temperature. The mean grain size is 141 μm and dislocation density is less than 10^{12}m^{-2} . The APT analysis of the as-received state confirmed the homogeneous distribution of Cr atoms with a composition of 15.05 ± 0.02 at.% Cr [18].

Massive disc-like shape samples of 100 μm thick and 3 mm of diameter were first mechanically polished and then electro-chemically polished in a solution of 10% perchloric acid, 20% Butoxy–2 ethanol and 70% ethanol absolute ($T = 5^\circ\text{C}$, $V \approx 30 \text{V}$) in order to remove plastic deformation introduced during mechanical polishing. They were irradiated with 2 MeV Fe^{2+} ions at 300°C using the JANNuS-Saclay facility [28,29]. The irradiation temperature was measured with three thermocouples and an infrared camera. The ion flux, measured with six faraday cup, was 5.4×10^{10} ions/($\text{cm}^2 \cdot \text{s}$). The damage and implantation profiles, given in Figure 1, were calculated with SRIM (Stopping and Range of Ions in Matter) [30,31] using the ‘Quick’ Kinchin and Pease option, as recommended by Stoller et al. [32], and a displacement threshold of 40 eV [33]. The dose rate varied from 3×10^{-5} dpa/s near the surface up to 6.1×10^{-5} dpa/s at the damage peak.

The APT samples were lifted out using a Helios 650 NanoLab FEI-focused ion beam at different depths in order to characterise α' precipitation with respect to the damage and implantation profiles. The final milling was performed with a Ga beam energy of 2 kV in order

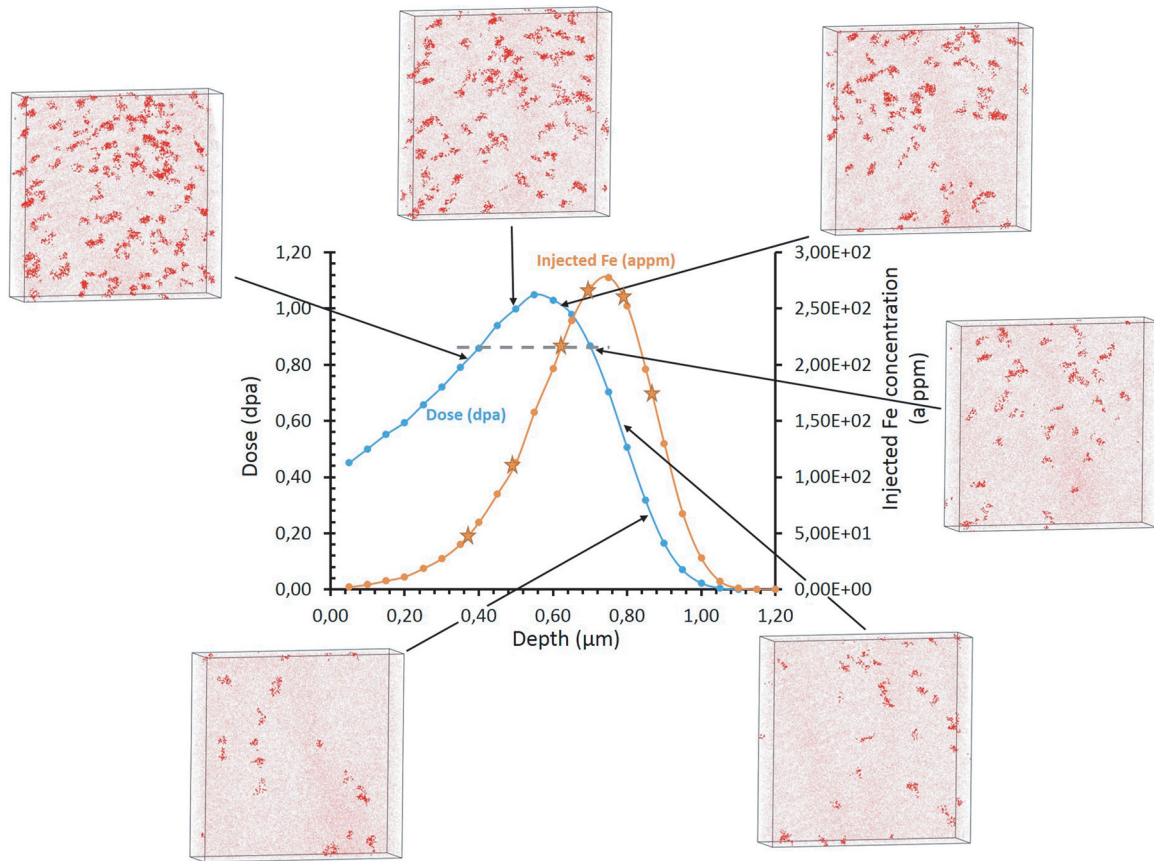


Figure 1. Damage and implantation profiles calculated with SRIM 2013 [30,31] and the 3D distribution of Cr atoms observed using APT at different depths (i.e. doses). A concentration threshold of $X_{Cr} > 24\text{at.}\%$ was used to highlight α' particles. APT volume $V = 40 \times 40 \times 10 \text{ nm}^3$, α' radius $r \approx 1 \text{ nm}$.

to reduce implantation of Ga ions in the material. The samples were analysed using a LEAP 4000X HR Atom Probe from CAMECA having a high mass resolution ($(M/\Delta M)_{1\%} = 233$ for the major peak of Fe) and a detector efficiency of 42%. The samples were cooled down to a temperature of 55 K in order to mitigate the preferential field evaporation of Cr atoms. During analyses, the atom probe specimens were electrically pulsed with a pulse fraction of 20%, a pulse rate of 200 kHz and a detection rate of 0.003 atom per pulse. Reconstructions of the volumes were done with IVAS 3.6.8 (CAMECA software) using the same parameters as in [18]: a compression factor of 1.4–1.5, an evaporation field of 33 V.nm^{-1} and a k factor of 3.25–4.5.

Data treatments were performed thanks to the 3D Data Software for APT developed by the GPM research group in Rouen, France. Measurement of the size and number density of clusters were performed using the ‘iso-position’ concentration data filter [10,34]. The filter enables to distinguish the particles from the surrounding matrix owing to their chemical composition. The parameters used were: concentration threshold $X_{Cr} > 24 \text{ at.}\%$, grid pattern of 0.8 nm, separation distance $d = 0.2 \text{ nm}$

and a minimum number of atoms in the particles of 80. The cluster composition was measured in the core of each cluster to eliminate the compositional dependence on the threshold value. Composition values were averaged over all the measurements. The number density of the particles was determined by a simple ratio of the number of observed precipitates to the overall analysed volume. The radius of each precipitate was deduced from the number of Cr and Fe atoms in each particle considering spherical particles: $R = \sqrt[3]{3nV_{\text{at}}/4\pi Q}$ with V_{at} the Fe atomic volume and Q the detector efficiency. The volume fraction was defined as the ratio of the number of atoms inside the precipitates to the total number of collected atoms. The basic principle of APT and data treatment may be found in different books or reviews [35–38].

Figure 1 plots both damage and injected Fe concentration profiles obtained under Fe^{2+} ion irradiation. The 3D distributions of Cr atoms observed with APT from 300 to 900 nm in depth are also presented. The first noticeable point is that α' particles formed. To the best of our knowledge, it is the first time that α' precipitation is observed under heavy ion irradiation. This clearly proves that α' particles can be observed under self-ion irradiation with

a dose rate of $\sim 10^{-5}$ dpa/s at 300°C. These results confirm that ballistic dissolution does not occur at this dose rate and irradiation temperature.

The evolution with depth of the particle radius, number density, volume fraction and of the Cr concentration both in the particles and in the matrix is given in Figure 2. Figures 1 and 2 clearly reveal that the advance of the α' precipitation is depth dependant. The number density and the volume fraction of α' particles are eight times higher at low depth than at 800 nm and deeper. The Cr content of α' particles is 10at.% higher below 350 nm than

at depth greater than after about 800 nm. From about 800 nm, the Cr content of the α matrix is close to its nominal level, whereas it decreases down to 13.8 at.% below 350 nm. The behaviour of the radius is less depth sensitive. The evolution may show a slight decrease. Nevertheless, judged by uncertainties and the small variation of the radius, it is not possible to conclude that the evolution is significant. Note that as under electron irradiation [18], C contamination during irradiation was measured with APT (between 0.02 and 0.08 at.% as under electron irradiation). C was homogeneously distributed. Most of

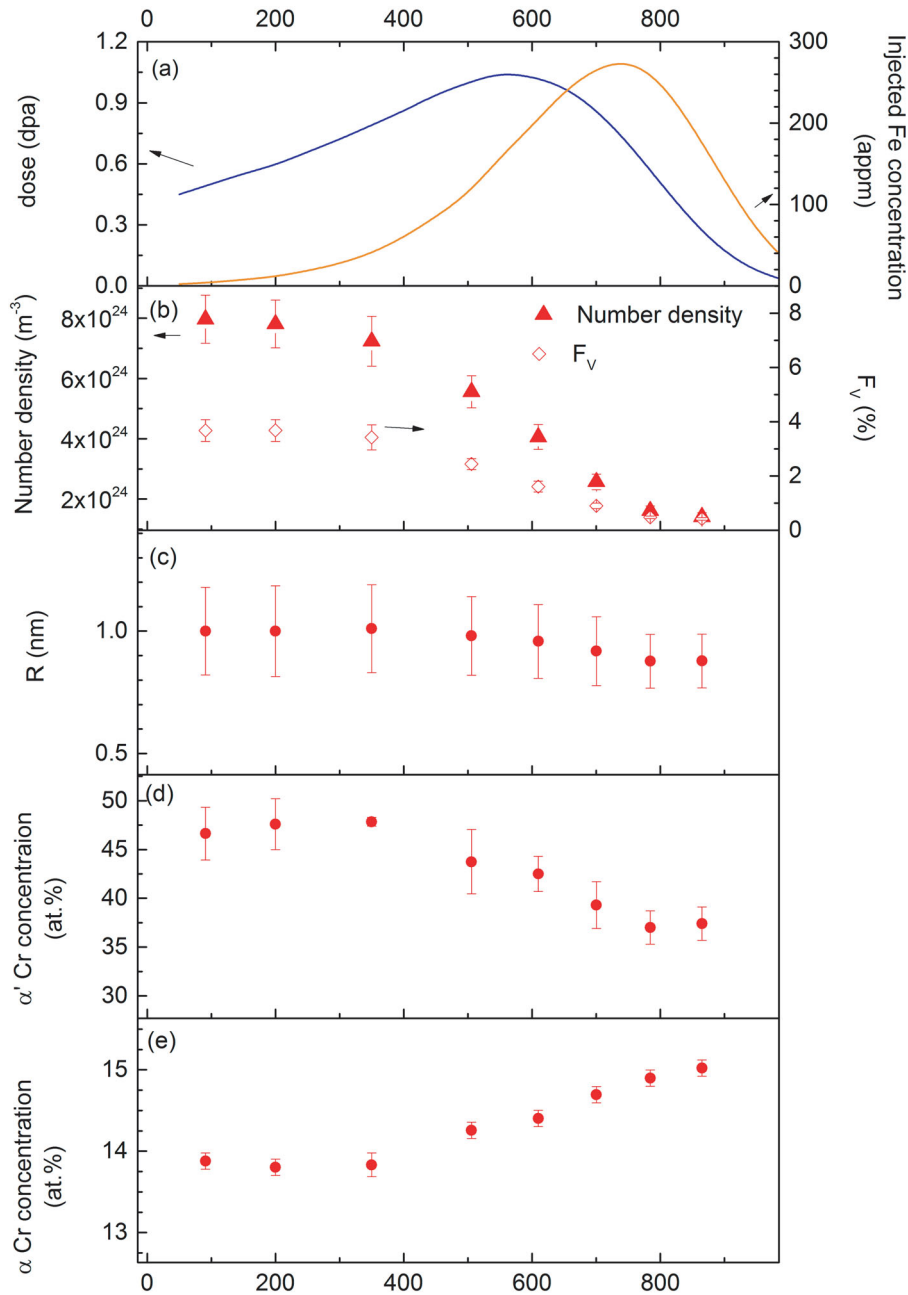


Figure 2. Evolution with irradiation depth of (a) damage and injected Fe concentration, (b) the particle number density and volume fraction, (c) the mean particle radius, Cr concentration in (d) particles and (e) α matrix. The alloy investigated is a Fe-15at.%Cr alloy irradiated with 2 MeV Fe^{2+} ions at 300°C.

α' precipitates do not include any C atoms. Clearly, the Cr-rich particles observed are α' particles, not carbides.

Regarding the evolution of the different characteristics of the α/α' decomposition, the figures are roughly constant up to about 350 nm. From 350 nm, α' decomposition becomes less developed moving deeper in the irradiated material. Maximum decomposition is not observed at the peak damage region (550 nm). It is also worth noting that the two 3D distributions of Cr atoms observed at 400 and 700 nm (dashed line in Figure 1) are significantly different, whereas they were obtained at the same dose (0.85 dpa). It is a clear evidence of the injected interstitial effect. Undoubtedly, the evolution of α' precipitation deviates significantly from that expected from the damage profile. Figure 2 clearly shows that the depth dependence of α/α' decomposition is correlated with the evolution of the injected Fe concentration rather than the damage profile. This behaviour is similar to that observed in the case of void formation [23,24,26,27]. When the contribution of injected Fe becomes more significant, the decomposition decreases. The origin of this behaviour can be explained as follows. The excess of interstitials due to injected Fe has two major effects: the enhancement of recombination between vacancies and interstitials and the creation of a high density of point defect sinks (interstitial clusters, dislocation loops). Both effects lead to a significant decrease in the concentration of the vacancies required for the diffusion of Cr atoms to form α' precipitates. Consequently, α' precipitation kinetics is reduced. Investigation and characterisation of the influence of injected Fe on the evolution of the matrix damage are ongoing.

This work shows that injected Fe reduced α' precipitation. This suggests that α' precipitation should be unlikely to occur if the concentration of injected Fe becomes high. This can explain why α' precipitation was not observed in [10]. In these experiments, a three-step irradiation with 0.5, 2 and 5 MeV Fe ions was applied to Fe-9at.%Cr and Fe-12at.%Cr alloys in order to obtain a flat damage profile. Nevertheless, the multi-step irradiation does not only flatten the damage profile but also the injected Fe concentration profile. A non-negligible concentration of injected ions was thus introduced over the whole irradiation depth probably preventing α' precipitation. In addition, a flux effect could also be involved. Indeed, the dose rate used in our work is low for heavy ions irradiation. Such a low-dose rate might be a necessary condition for the formation of α' particles. However, the damage rate difference between [10] and the present case is no larger than a factor of 5, which is quite small. Its influence is probably not so important. Nevertheless, this point is under investigation.

Also, quite often, microstructural investigations are conducted at peak damage in order to investigate irradiation effects at high doses. However, while the dose is higher in the peak region, so is the concentration of injected ions. Our results show that such investigation of α' precipitation at the damage peak is not appropriate.

In the depth range of 90–350 nm, a plateau is observed where the dose rises from 0.5 to 0.8 dpa. The absence of increase in α/α' decomposition in this range might be the signature of the beginning of the influence on the microstructure evolution of the injected Fe ions and their long range diffusion in the concentration gradient. Moreover, the fact that α' particles are observed at 90 nm is not enough to rule out some possible surface effect (efficient loss of point defects at the surface) on the microstructure. Consequently, α' precipitation characteristics observed in the plateau might be biased by surface effect on the one hand and injected Fe on the other hand. It is not possible to know whether there exists a region where no artefact due to ion irradiation occurs. Experiments performed with higher ions energies, for instance, 5 or 10 MeV, should enable to characterise a region deep enough to avoid surface effects and far enough from the implantation peak to study α' precipitation.

In conclusion, this paper was aimed at explaining the origin of the absence of α' precipitation under ion irradiation. It presents an APT investigation of a Fe-15at.%Cr alloy irradiated with 2 MeV Fe²⁺ ions at 300°C. The 3D distribution of Cr atoms revealed the presence of α' particles. To the best of our knowledge, it is the first time that α' precipitation is observed under heavy ion irradiation. Characterisation of α/α' decomposition with depth and comparison with both the damage and injected Fe concentration profiles show that:

- Evolution of α' precipitation deviates significantly from that is expected from the damage profile.
- Injected Fe strongly reduced α' precipitation.

According to these results, the absence of α' precipitates in previous ion irradiation experiments is likely due to the presence of a high concentration of injected interstitials because of the use of multi-step irradiations, very high-dose rates or investigation at the damage peak. Multi-step ion irradiations or characterisation at the damage peak in order to reach high irradiation doses are thus not recommended.

Acknowledgements

The authors acknowledge A. Barbu and F. Soisson for fruitful simulating discussions.

Disclosure statement

No potential conflict of interest was reported by the authors.

Funding

The research was partly supported by the 'défi NEEDS' (CNRS-CEA-EDF-ANDRA-AREVA-IRSN-BRGM) within the project ETIC. It also contributes to the EC project MatISSE (Grant Agreement No. 604862) and to the Joint Programme on Nuclear Materials of EERA. The experiments were done using the triple beam facility at the CEA Saclay, France and supported by the French Network EMIR and Eurofusion.

References

- [1] Klueh RL, Harries DR. High-chromium ferritic and martensitic steels for nuclear application. West Conshohocken: ASTM; 2001.
- [2] Garner F, Toloczko M, Sencer B. Comparison of swelling and irradiation creep behavior of fcc-austenitic and bcc-ferritic/martensitic alloys at high neutron exposure. *J Nucl Mater.* 2000;276:123–142.
- [3] Little EA. Development of radiation resistant materials for advanced nuclear power plant. *Mater Sci Technol.* 2006;22:491–518.
- [4] Yvon P, Carré F. Structural materials challenges for advanced reactor systems. *J Nucl Mater.* 2009;385:217–222.
- [5] Murty KL, Charit I. Structural materials for Gen-IV nuclear reactors: challenges and opportunities. *J Nucl Mater.* 2008;383:189–195.
- [6] Kohyama A, Hishinuma A, Gelles D, et al. *J Nucl Mater.* 1996;233–237:138–147.
- [7] Matijasevic M, Almazouzi A. Effect of Cr on the mechanical properties and microstructure of Fe–Cr model alloys after n-irradiation. *J Nucl Mater.* 2008;377:147–154.
- [8] Was GS, Averback RS. 1.07—radiation damage using ion beams A2—Konings. Rudy J.M. *Compr. Nucl. Mater.* [Internet]. Oxford: Elsevier; 2012 [cited 2016 Apr 26]. p. 195–221. Available from: <http://www.sciencedirect.com/science/article/pii/B9780080560335000070>
- [9] Kuksenko V, Pareige C, Pareige P. Cr precipitation in neutron irradiated industrial purity Fe–Cr model alloys. *J Nucl Mater.* 2013;432:160–165.
- [10] Pareige C, Kuksenko V, Pareige P. Behaviour of P, Si, Ni impurities and Cr in self ion irradiated Fe–Cr alloys—comparison to neutron irradiation. *J Nucl Mater.* 2015;456:471–476.
- [11] Kuksenko V, Pareige C, Génévois C, et al. Effect of neutron-irradiation on the microstructure of a Fe–12at.%Cr alloy. *J Nucl Mater.* 2011;415:61–66.
- [12] Bergner F, Pareige C, Kuksenko V, et al. Critical assessment of Cr-rich precipitates in neutron-irradiated Fe–12at.%Cr: comparison of SANS and APT. *J Nucl Mater.* 2013;442:463–469.
- [13] Heintze C, Bergner F, Ulbricht A, et al. The microstructure of neutron-irradiated Fe–Cr alloys: a small-angle neutron scattering study. *J Nucl Mater.* 2011;409:106–111.
- [14] Bachhav M, Robert Odette G, Marquis EA. Microstructural changes in a neutron-irradiated Fe–15 at.%Cr alloy. *J Nucl Mater.* 2014;454:381–386.
- [15] Bachhav M, Robert Odette G, Marquis EA. A' precipitation in neutron-irradiated Fe–Cr alloys. *Scr Mater.* 2014;74:48–51.
- [16] Chen W-Y, Miao Y, Wu Y, et al. Atom probe study of irradiation-enhanced α' precipitation in neutron-irradiated Fe–Cr model alloys. *J Nucl Mater.* 2015;462:242–249.
- [17] Jiao Z, Shankar V, Was GS. Phase stability in proton and heavy ion irradiated ferritic–martensitic alloys. *J Nucl Mater.* 2011;419:52–62.
- [18] Tissot O, Pareige C, Meslin E, et al. Kinetics of α' precipitation in an electron-irradiated Fe15Cr alloy. *Scr Mater.* 2016;122:31–35.
- [19] Soisson F, Jourdan T. Radiation-accelerated precipitation in Fe–Cr alloys. *Acta Mater.* 2016;103:870–881.
- [20] Garner FA. Impact of the injected interstitial on the correlation of charged particle and neutron-induced radiation damage. *J Nucl Mater.* 1983;117:177–197.
- [21] Plumton DL, Attaya H, Wolfer WG. Conditions for the suppression of void formation during ion-bombardment. *J Nucl Mater.* 1984;122:650–653.
- [22] Brailsford AD, Mansur LK. Effect of self-ion injection in simulation studies of void swelling. *J Nucl Mater.* 1977;71:110–116.
- [23] Lee EH, Mansur LK, Yoo MH. Spatial variation in void volume during charged particle bombardment—the effects of injected interstitials. *J Nucl Mater.* 1979;85:577–581.
- [24] Plumton DL, Wolfer WG. Suppression of void nucleation by injected interstitials during heavy ion bombardment. *J Nucl Mater.* 1984;120:245–253.
- [25] Bullen DB, Kulcinski GL, Dodd RA. Swelling suppression by injected self-interstitials. *Nucl Instrum Methods Phys Res Sect B Beam Interact Mater At.* 1985;10:561–564.
- [26] Shao L, Wei C-C, Gigax J, et al. Effect of defect imbalance on void swelling distributions produced in pure iron irradiated with 3.5 MeV self-ions. *J Nucl Mater.* 2014;453:176–181.
- [27] Bhattacharya A, Meslin E, Henry J, et al. *Acta Mater.* 2016; submitted.
- [28] Serruys Y, Trocellier P, Miro S, et al. JANNUS: a multi-irradiation platform for experimental validation at the scale of the atomistic modelling. *J Nucl Mater.* 2009;386–388:967–970.
- [29] Beck L, Serruys Y, Miro S, et al. Ion irradiation and radiation effect characterization at the JANNUS-saclay triple beam facility. *J Mater Res.* 2015;30:1183–1194.
- [30] Ziegler JF, Ziegler MD, Biersack JP. SRIM—The stopping and range of ions in matter (2010). *Nucl Instrum Methods Phys Res Sect B Beam Interact Mater At.* 2010;268:1818–1823.
- [31] Ziegler JF, Biersack JP, Littmark U. The stopping and range of ions in matter. New York: Pergamon Press; 1985.
- [32] Stoller RE, Toloczko MB, Was GS, et al. On the use of SRIM for computing radiation damage exposure. *Nucl Instrum Methods Phys Res Sect B Beam Interact Mater At.* 2013;310:75–80.
- [33] ASTM E693. Annu. Book ASTM Stand. 1994;12.02.
- [34] Meslin E, Radiguet B, Loyer-Prost M. Radiation-induced precipitation in a ferritic model alloy: an experimental and theoretical study. *Acta Mater.* 2013;61:6246–6254.

- [35] Larson DJ, Prosa TJ, Ulfig RM, et al. Local electrode atom probe tomography [Internet]. New York, NY: Springer New York; 2013 [cited 2016 Apr 26]. Available from: <http://link.springer.com/10.1007/978-1-4614-8721-0>
- [36] Moody MP, Cairney JM, Gault B, et al. Atom probe microscopy [Internet]. Springer Series in Materials Science, vol. 160. 2012 [cited 2012 Oct 24]. Available from: <http://www.springer.com/materials/characterization+%26+evaluation/book/978-1-4614-3435-1>
- [37] Miller M, Cerezo A, Hetherington M, et al. Atom probe field ion microscopy. Press C, editor. Clarendon: Oxford; 1996.
- [38] Miller M. Atom probe tomography. New York: Kluwer Academic/Plenium; 2000.